

# A near-infrared methane detection system using a 1.654 $\mu\text{m}$ wavelength-modulated diode laser\*

FU Yang (付洋)<sup>1</sup>, LIU Hui-fang (刘慧芳)<sup>1</sup>, SUI Yue (隋越)<sup>1</sup>, LI Bin (李彬)<sup>1</sup>, YE Wei-lin (叶玮琳)<sup>2</sup>, ZHENG Chuan-tao (郑传涛)<sup>1\*\*</sup>, and WANG Yi-ding (王一丁)<sup>1</sup>

1. State Key Laboratory on Integrated Optoelectronics, College of Electronic Science and Engineering, Jilin University, Changchun 130012, China

2. College of Engineering, Shantou University, Shantou 515063, China

(Received 5 December 2015)

©Tianjin University of Technology and Springer-Verlag Berlin Heidelberg 2016

By adopting a distributed feedback laser (DFBL) centered at 1.654  $\mu\text{m}$ , a near-infrared (NIR) methane ( $\text{CH}_4$ ) detection system based on tunable diode laser absorption spectroscopy (TDLAS) is experimentally demonstrated. A laser temperature control as well as wavelength modulation module is developed to control the laser's operation temperature. The laser's temperature fluctuation can be limited within the range of  $-0.02$ – $0.02$   $^\circ\text{C}$ , and the laser's emitting wavelength varies linearly with the temperature and injection current. An open reflective gas sensing probe is realized to double the absorption optical path length from 0.2 m to 0.4 m. Within the detection range of 0–0.01, gas detection experiments were conducted to derive the relation between harmonic amplitude and gas concentration. Based on the Allan deviation at an integral time of 1 s, the limit of detection ( $LoD$ ) is decided to be  $2.952 \times 10^{-5}$  with a path length of 0.4 m, indicating a minimum detectable column density of  $\sim 1.2 \times 10^{-5}$  m. Compared with our previously reported NIR  $\text{CH}_4$  detection system, this system exhibits some improvement in both optical and electrical structures, including the analogue temperature controller with less software consumption, simple and reliable open reflective sensing probe.

**Document code:** A **Article ID:** 1673-1905(2016)02-0140-4

**DOI** 10.1007/s11801-016-5243-y

The detection on methane ( $\text{CH}_4$ ) concentration becomes significant, and numerous technologies have been employed<sup>[1-4]</sup>. As an infrared (IR) absorption spectroscopy technique, the tunable diode laser absorption spectroscopy (TDLAS) is widely used in the field of trace gas detection<sup>[5-7]</sup>. In order to suppress noises and achieve high signal-to-noise ratio ( $SNR$ ), the wavelength modulation spectroscopy (WMS) technology is broadly adopted in gas detection<sup>[8,9]</sup>. Thus, IR  $\text{CH}_4$  detection has been widely reported by numerous groups based on the combined technology of TDLAS-WMS<sup>[10-12]</sup>. Generally, the performance of a distributed feedback laser (DFBL)-based  $\text{CH}_4$  detection system is restricted by the stability of DFBL's emitting wavelength, effective absorption length, and the performance of the used lock-in amplifier. Different from our previous reports<sup>[13,14]</sup>, in this paper, an analog-circuit-based PID network is applied in the laser temperature control module. In this way, the relative software consumption can be reduced, and the control stability on temperature is improved from  $\pm 0.1$   $^\circ\text{C}$  to  $\pm 0.02$   $^\circ\text{C}$ . An open reflective gas sensing

probe was developed to double the absorption optical path length from 0.2 m to 0.4 m. Besides, since the sensing probe is exposed to open air, the response time of the system can also be shortened. Consequently, the system structure has been simplified, and the overall performance has been improved.

The schematic of this TDLAS-based  $\text{CH}_4$  detection system is shown in Fig.1. A 14-pin butterfly-packaged DFBL and an open reflective sensing probe are included. The whole system is divided into three sections. The first section is DFBL driver, including a microcontroller (MCU0, TMS320F28335), a laser current controller as well as a temperature controller. The modulated DFBL generates an optical light beam with the wavelength around 1.654  $\mu\text{m}$ . For the second optical module (OM) section, the optical beam firstly reaches a fiber optic beam splitter (FOBS) and is split into two beams with equal power. One beam propagates through the reflective probe that is placed inside the gas cell to generate an absorption signal ( $u_i(t)$ ) via a detector, and the other one transmits through an optical attenuator (OA) to generate

\* This work has been supported by the National Key Technology R&D Program of China (Nos.2013BAK06B04 and 2014BAD08B03), the National Natural Science Foundation of China (Nos.61307124 and 11404129), the Science and Technology Department of Jilin Province of China (Nos.20120707 and 20140307014SF), the Changchun Municipal Science and Technology Bureau (Nos.11GH01 and 14KG022), and the State Key Laboratory on Integrated Optoelectronics, Jilin University (No.IOSKL2012ZZ12).

\*\* E-mail: zhengchuantao@jlu.edu.cn

a reference signal ( $u_r(t)$ ) via another detector. These two signals correspond to channel 1 (C1) signal and channel 2 (C2) signal, respectively. A subtraction is performed on the two signals by a specific circuit in the third section, i.e., signal processing module (SPM). The subtraction result is input into an orthogonal lock-in amplifier, and then two orthogonal analogue components are generated. After that, an analog-to-digital converter (ADC) as well as another digital signal processor (DSP) (MCU1, TMS320F28335) is used to convert the two analogue signals into digital ones for obtaining the  $2f$  harmonic signals. Finally, the MCU1 presents the detected concentration through a liquid crystal display (LCD). Generally, the amplitude of the  $2f$  signal ( $Amp[A_{2f}(t)]$ ) is related to  $CH_4$  concentration, which can be expressed as

$$Amp[A_{2f}(t)] = F(C), \tag{1}$$

where the expression of  $F$  can be achieved through calibration experiment.

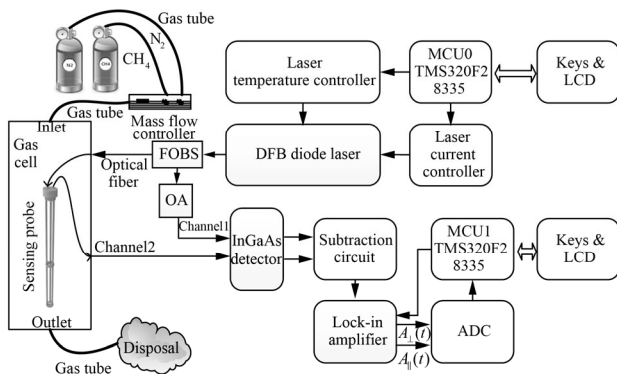


**Fig.1 Configuration of the near-infrared  $CH_4$  detection system using DFBL at  $1.654 \mu m$**

The 14-pin butterfly-packaged DFBL applied in this detection system was fabricated by Institute of Semiconductors, Chinese Academy of Sciences. The center emitting wavelength of the laser is around  $1.654 \mu m$ . A negative temperature coefficient (NTC) thermistor and a thermoelectric cooler (TEC) are packaged inside the laser for temperature monitoring and controlling. At  $25 \text{ }^\circ C$ , its threshold current is  $17.23 \text{ mA}$ , and its output optical power is  $5.34 \text{ mW}$  at an injection current of  $60 \text{ mA}$ . Normally, the laser's driving current is set to be within the range of  $40\text{--}80 \text{ mA}$ . Besides, two InGaAs photodiodes (J23-18I-R01M-2.2, Teledyne Judson Technologies) with a spectral range of  $0.8\text{--}2.2 \mu m$  are used to convert the infrared light power into the reference signal and the absorption signal.

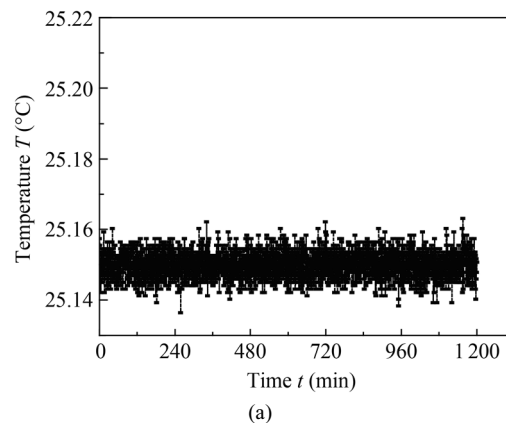
Temperature control of the DFBL is crucial for  $CH_4$  detection, due to the fact that the laser's central wavelength depends on the laser's operation temperature. Based on Peltier effect, the laser's temperature can be set through a TEC module, which is integrated in the DFBL. The DFBL's real-time temperature can be obtained by an inside-packaged thermistor with NTC. With a digi-

tal-to-analog converter (DAC, AD5060), the DSP generates an analog voltage signal to the TEC controller to set a needed temperature. A highly-efficient and reliable monolithic TEC controller, ADN8831, is used to drive the TEC. It sets the laser's temperature in a programmable way and maintains the stable temperature by using an analog PID control loop. There are several key-buttons that are programmed to trigger specific functions, e.g., modifying laser temperature.

Experiments were carried out to investigate the performance of the temperature controller. Fig.2(a) shows the stability of the temperature control module during an operation period for 20 h, where the temperature was set to be  $25.15 \text{ }^\circ C$ . A random period of 100 min is selected to see the details, as shown in Fig.2(b). It can be seen that the practical operation temperature varies within the range of  $\pm 0.01 \text{ }^\circ C$ , which is small enough to avoid the fluctuation of emitting wavelength. With a constant driving current of  $70 \text{ mA}$ , we measured the emitting spectrum of the laser with increasing the temperature. The higher the operation temperature is, the larger the peak emitting wavelength becomes, which proves good stability and linearity of the developed temperature controller.

For the developed DFBL driver, a saw-wave scan signal of  $10 \text{ Hz}$  is generated by a DAC device (AD5541). Meanwhile, a direct digital synthesizer (DDS, AD9851) is utilized to generate a  $5 \text{ kHz}$  sine-wave modulation signal. These two signals combine together and both act on the laser's output. Then, a voltage-controlled constant current source (VCCS) module is used to convert the voltage signal into current signal for driving the DFBL directly. Experiments were carried out to investigate the driving performance along with the operation of temperature control module. With different temperatures, curves of the laser's emitting peak wavelength versus its injection current are shown in Fig.2(c). It can be seen that the emitting peak wavelength increases linearly with the rising current with certain operation temperatures.

Detailed structure and picture of the used open reflective sensing probe are shown in Fig.3. Two FC/APC fiber interfaces/connectors are used as input and output ports for receiving the incident light beam and the reflected light beam, respectively. There is a mirror located



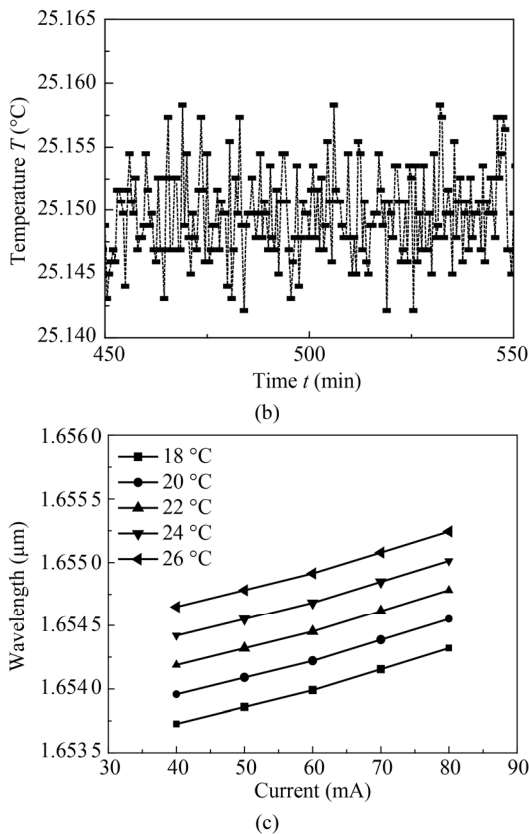


**Fig.2 (a)** With the operation of the developed intelligent temperature controller, the measured temperature of the DFBL for 20 h, where the operation temperature is set to be 25.15 °C; **(b)** The detailed measured temperature within a random period of 100 min; **(c)** With different operation temperatures, the emitting peak wavelength versus injection current

at the bottom to double the path length by reflecting the input optical beam, which comes from one branch of the FOBS, to the pre-adjusted output port. During detection, the NIR light propagates through a certain amount of CH<sub>4</sub> in the open air and is absorbed by CH<sub>4</sub> molecule.

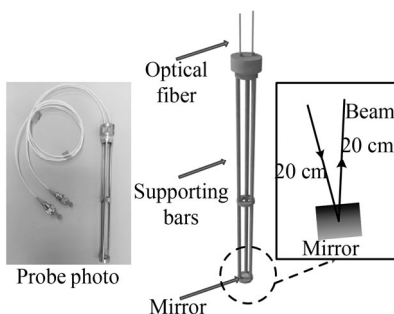


**Fig.3 Structure and picture of the open reflective gas sensing probe**

By mixing different amounts of CH<sub>4</sub> and N<sub>2</sub>, standard gas samples can be prepared. Within the concentration range of 0—0.01, the measured amplitude of the 2f signal is shown in Fig.4. The obtained relation between CH<sub>4</sub>

concentration and 2f amplitude is

$$Amp[A_{2f}(t)] = 1\,749.07 + 0.040\,81C(\text{mV}), 0 \leq C \leq 0.01 \quad (2)$$

It has been seen from experiment that as the concentration is below  $6 \times 10^{-4}$  or lower (see the inset in Fig.4), the harmonic signal will be partially or absolutely buried in noises, which makes it hard to decide the harmonic amplitude.

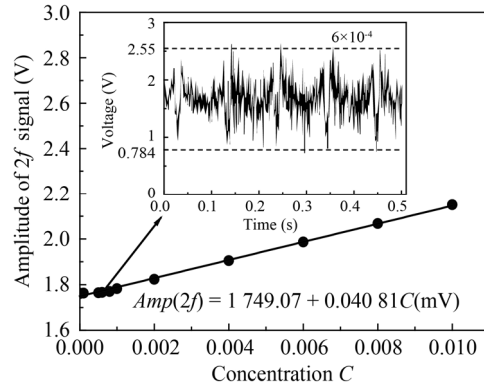


**Fig.4** Within the concentration range of 0—0.01, the measured amplitude of 2f signal (The inset shows the 2f harmonic signal with the CH<sub>4</sub> concentration of  $6 \times 10^{-4}$ .)

In order to accurately determine the LoD of the system, we measured the amplitude of the 2f signal in N<sub>2</sub> atmosphere for a period of 3 000 s, as shown in Fig.5(a). It can be seen that the 2f signal amplitude is within the range of 1 748—1 752 mV. Using Eq.(2), we derive the concentration variation, which is also shown in Fig.5(a). Fig.5(b) shows the Allan deviation curve of the detection system, where the integral time is within the range of 1—700 s. One can determine that with 1 s integral time, the Allen deviation value of the system is about  $2.952 \times 10^{-5}$ , which is almost equal to the standard deviation (SD) of  $3.12 \times 10^{-5}$ . The system shows the best stability with an integral time of about 40—70 s, and the corresponding Allen deviation value is about  $5 \times 10^{-6}$ .

Here, we define two kinds of LoDs, the first one, expressed as LoD<sub>1</sub>, is equal to the Allan deviation value with the integral time of 1 s, i.e., LoD<sub>1</sub> =  $2.952 \times 10^{-5}$ , and the second one, expressed as LoD<sub>3</sub>, is defined as 3 times of the standard deviation of the measured concentration, i.e., LoD<sub>3</sub> =  $3 \times 3.12 \times 10^{-5} = 9.36 \times 10^{-5}$ . Traditionally, we use LoD<sub>1</sub> (Allan deviation with 1 s integral time) to represent the LoD of the system. Since the absorption length is about 0.4 m, a minimum detectable column density of  $2.952 \times 10^{-5} \times 0.4 \text{ m} = 1.18 \times 10^{-5} \text{ m}$  is achieved through experiment. The LoD can be further decreased by the following measures: increasing the path length of the gas sensing probe; narrowing the detection range; using some effective digital method to process the signal before extracting the amplitude. Despite this, such properties are sufficient in the detection of CH<sub>4</sub> in mine environment.

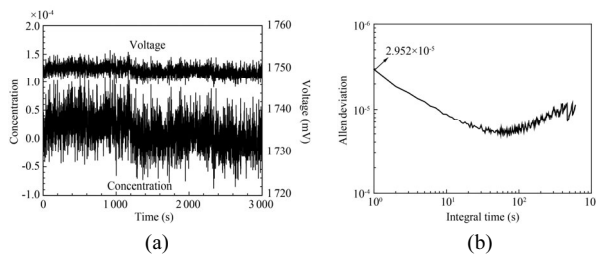


**Fig.5 (a) The amplitude of the 2f signal and concentration variation in N<sub>2</sub> atmosphere for a period of 3 000 s; (b) The Allan deviation curve of the detection system**

A comparison is made among the performances of this CH<sub>4</sub> detection system and other two CH<sub>4</sub> sensors, including the handheld battery-powered TDL sensor<sup>[15]</sup> and the natural gas pipeline NIR leak detector<sup>[16]</sup>. It can be seen that the used lasers and detectors for the three sensors are generally the same. The proposed sensor and that reported in Ref.[15] are based on DSP and self-developed laser drivers and lock-in amplifiers, so they are more portable with small size and low cost for field CH<sub>4</sub> detection. The three sensors, especially this sensor and the one reported in Ref.[15], also show a similar level in the minimum detectable column density, because of the use of similar absorption line at 1.65 μm and similar InGaAs detectors.

**Tab.1 Comparison among this CH<sub>4</sub> sensor and other two reported sensors in Refs.[15,16]**

Sensor	Sensor type	Laser wavelength	Detector	Detectable column density
Ref.[15]	Portable	1.65 μm (not specify the line)	InGaAs detector (type is unavailable)	1.2×10 <sup>-5</sup> m
Ref.[16]	Not portable	1.653 7 μm (2ν <sub>3</sub> band, R3 line)	InGaAs detector (type is unavailable)	5×10 <sup>-5</sup> m
This paper	Portable	1.653 7 μm (2ν <sub>3</sub> band, R3 line)	InGaAs detector (J23-18I-R01M-2.2)	1.18×10 <sup>-5</sup> m

In conclusion, based on TDLAS technique, a CH<sub>4</sub> detection system was experimentally demonstrated, which adopts a DFBL, an open reflective gas sensing probe and two InGaAs photodiodes. With the operation of the developed DFBL driver, the laser temperature fluctuation can be limited to the range of -0.02—0.02 °C, and the laser’s emitting wavelength varies linearly with the temperature and injection current. The developed orthogonal lock-in amplifier can effectively extract the 1f and 2f harmonic signals. As the CH<sub>4</sub> concentration increases from 0 to 0.01, the amplitudes of the 2f harmonic signals

are obtained. Based on the Allan deviation at an integral time of 1 s, the *LoD* is decided to be 2.952×10<sup>-5</sup> with a path length of 0.4 m, indicating a minimum detectable column density of 1.2×10<sup>-5</sup> m. Compared with our previously reported NIR CH<sub>4</sub> detection system, this system exhibits some improvement in both optical and electrical structures, including the analogue temperature controller with small software consumption, the open reflective gas sensing probe with fast response speed, etc.

**References**

- [1] Y. Cao, N. Sanchez, W. Jiang, R.J. Griffin, F. Xie, L.C. Hughes, C. Zah and F.K. Tittel, *Optics Express* **23**, 2121 (2015).
- [2] W.L. Ye, C.T. Zheng and Y.D. Wang, *Journal of Optoelectronics-Laser* **26**, 1030 (2015). (in Chinese)
- [3] G.Z. Gao, B.X. Chen, B. Hu, T.J. Jia and H.H. Yi, *Journal of Optoelectronics-Laser* **25**, 718 (2014). (in Chinese)
- [4] Q. Gao, Y. Zhang, J. Yu, S. Wu, Z. Zhang, F. Zheng, X. Lou and W. Guo, *Sensors and Actuators A: Physical* **199**, 106 (2013).
- [5] M. Wolff, S. Rhein, H. Bruhns, L. Nähle, M. Fischer and J. Koeth, *Sensors and Actuators B: Chemical* **187**, 574 (2013).
- [6] F. Wang, Q. Wu, Q. Huang, H. Zhang, J. Yan and K. Cen, *Optics Communications* **346**, 53 (2015).
- [7] W. Wei, J. Chang, Q. Huang, C. Zhu, Q. Wang, Z. Wang and G. Lv, *Applied Physics B: Lasers and Optics* **118**, 75 (2015).
- [8] R. Sur, K. Sum, J.B. Jeffries, J.G. Socha and R.K. Hanson, *Fuel* **150**, 102 (2015).
- [9] S.H. Salati and A. Khorsandi, *Applied Physics B: Lasers and Optics* **116**, 521 (2014).
- [10] R. Sur, K. Sun, J.B. Jeffries, R.K. Hanson, R.J. Pummill, T.Waind, D.R. Wagner and K.J. Whitty, *Applied Physics B: Lasers and Optics* **116**, 33 (2014).
- [11] W.L. Ye, C.T. Zheng, X. Yu, C.X. Zhao, Z.W. Song and Y.D. Wang, *Sensors and Actuators B: Chemical* **155**, 37 (2011).
- [12] Q. Wang, J. Chang, W. Wei, C. Zhu and C. Tian, *Applied Physics B: Laser and Optics* **117**, 1015 (2014).
- [13] C.T. Zheng, W.L. Ye, J.Q. Huang, T.S. Cao, M. Lv, J.M. Dang and Y.D. Wang, *Sensors and Actuators B: Chemical* **190**, 249 (2014).
- [14] C.T. Zheng, J.Q. Huang, W.L. Ye, M. Lv, J.M. Dang, T.S. Cao, C. Chen and Y.D. Wang, *Infrared Physics & Technology* **61**, 306 (2013).
- [15] R.T. Wainner, B.D. Green, M.G. Allen, M.A. White, J. Stafford-Evans and R. Naper, *Applied Physics B-Lasers and Optics* **75**, 249 (2002).
- [16] X. Gao, H. Fan, T. Huang, X. Wang, J. Bao, X. Li, W. Huang and W. Zhang, *Spectrochimica Acta Part A-Molecular and Biomolecular Spectroscopy* **65**, 133 (2006).